Presented at the 31st IEEE Photovoltaics Specialist Conference, Orlando Florida, January 3-7 2005.

QUANTUM DOT INTERMEDIATE BAND SOLAR CELL MATERIAL SYSTEMS WITH NEGLIGIBLE VALENCE BAND OFFSETS

Michael Y. Levy [1], Christiana Honsberg [2], Antonio Martí [3], Antonio Luque [3]

[1] School of Electrical and Computer Engineering, Georgia Institute of Technology, Atlanta, Georgia, 30332-0250, USA

[2] School of Electrical and Computer Engineering, University of Delaware, Newark, Delaware, 19716-3130, USA

[3] Instituto de Energia Solar - ETSIT, Universidad Politécnica de Madrid, Ciudad Universitaria sn, 28040 Madrid, Spain – EU

ABSTRACT

In this paper material triads (quantum-dot/barrier/substrate) are presented that may implement quantum dot intermediate band solar cells with conversion efficiencies greater than 60%. Triads whose barrier material and substrate material are lattice-matched are presented. In addition, triads are presented with the lattice constant of the substrate in-between the lattice constant of the barrier and the lattice constant of the quantum dot. The latter case provides triads that may remove strain during epitaxial growth.

INTRODUCTION

The objective of this article is to identify material systems that can be used to realize a quantum dot intermediate band solar cell (QD-IBSC). The operation of an intermediate band solar cell (IBSC) depends on a material with three bands: a conduction band (CB), a valence band (VB), and an intermediate band (IB) [1]. Due to the existence of three bands, there exist three bandgaps: a bandgap between the CB and VB, E_{CV}; a bandgap between the CB and IB, E_{CI}; and a bandgap between the IB and VB, E_{IV}. Each of these bands is associated with a distinct quasi-Fermi level. Under non-equilibrium conditions, three chemical potentials exist; one for each of the carrier populations associated with the three bandgaps. Due to increased photon-induced carrier generation, the existence of the IB provides more efficient solar energy conversion as compared to a single junction solar cell whose bandgap is equal in value to E_{CV} [1]. In order to provide high likelihood of carrier advancement to and from the IB, the Fermi level must exist near the IB.

The use of quantum dot (QD) technology is proposed as a near term proof of concept of the operating principles of an IBSC [2]. Quantum dot heterojunctions may implement an IBSC because of their ability to provide the three necessary bands. The chemical potential between the quantum dot intermediate band solar cell's CB and VB, μ_{CV}, is limited by the effective bandgap of the barrier material, $E_{G,B}$. The IB is created by a near period array of quantum dots of nearly uniform radii. Doping is employed in either the barrier material [3] or the quantum dot material [4] in order to ensure the proper placement of the Fermi level.

Two quantum dot heterojunction phenomena have been identified that need be avoided, at best, or mitigated, at least. These phenomena are the extension of the VB edge or CB edge into the formerly forbidden region of the barrier's bandgap [5], and the existence of more than one minibands (MB) between the CB and VB [5]. The extension into the previously forbidden bandgap results from electron or hole levels whose energies are near to (~4kT) the barrier's CB or VB respectively. This condition creates an overlap between the miniband and the CB or VB respectively. An example of such an extension is shown in Figure 1. Electron or hole levels whose energies are further from the band edges will form mini-bands between the CB and VB of the QD-IBSC. The theory of the IBSC mandates the existence of a single mini-band that is referred to as the IB. This miniband will be formed at an energy below the conduction band equal to the ground state energy $E_{1,0}$.

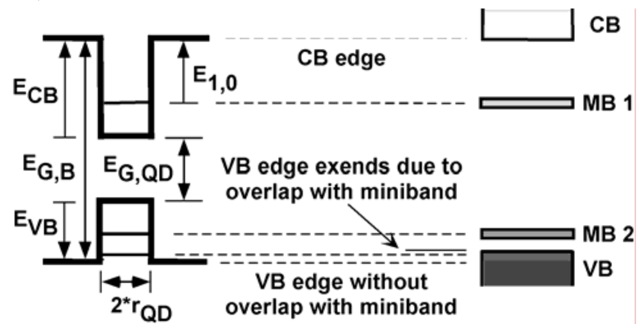

Fig. 1. Interpretation of the band structure of a periodic lattice of uniform quantum dots. On the left are the: CB offset, E_{CB}; VB offset, E_{VB}; bandgap of the barrier material, $E_{G,B}$; bandgap of the QD material, $E_{G,QD}$; and energy of the ground state electron, $E_{1,0}$, and hole energies that arise from the confining potentials of a QD of radius r_{QD}. On the right are the: CB; one MB formed from the ground state electron level; a second MB formed by the ground state hole level; and the VB. The VB edge extends into the previously forbidden bandgap due to an overlap with the MB associated with the first excited hole state.

The initial examination of the QD-IBSC explores a material system composed of InGaAs quantum dots enveloped in an AlGaAs barrier grown on a GaAs substrate [2]. This material triad is selected because of the large difference between the values of the quantum dot's bandgap and the barrier's bandgap. In addition, this triad is selected because it is a commonly fabricated and well characterized. The material systems with which to fabricate QD-IBSC that are presented in this article are chosen with the purpose of precluding the existence of hole levels and the reduced performance that the hole levels allow. Specifically, the triads are selected with negligible VB offsets.

QUANTUM DOT HETEROJUNCTIONS WITH NEGLIGABLE VALENCE BAND OFFSETS

The theory of semiconductor quantum dot superlattices, states that any allowed energy level that exists in a single quantum dot heterojunction will transform into a mini-band, with a given bandwidth, when many nearly uniform quantum dot heterojunctions are placed in a near periodic lattice. Allowed energy levels that are close to one another or close to the band edges of the barrier materials (within a few units of kT) may lead to a merging of two minibands or to a merging of a miniband with the either of barrier's bands. In the case where a miniband merges with the band edge of the barrier, the chemical potential, μ_{CV}, is reduced from the limiting chemical potential of the bulk barrier material, $\mu_{G,B}$. The existence of more than one miniband that does not merge with either of the barrier's bands is also problematic. This is the case because each miniband that does not contain a quasi-Fermi level located within it provides a greater likelihood of carrier recombination as compared with carrier generation. Figure 1 shows a hypothetical quantum dot heterojunction and its qualitative band structure.

Removing the confining potential of the holes or of the electrons will eliminate excess minibands. In this article, a decision is made to remove the confining potential of the holes by selecting a quantum dot heterojunctions with negligible valence band offsets. The justification for this choice is as follows. In most of the III-V semiconductor compounds the effective mass of the holes is greater than the effective mass of the electrons. In addition for the technologically realizable interval of quantum dot radii, for even a small valence band offset, many hole levels appear, whereas fewer electron energy levels appear. Thus within technologically realizable quantum dot radii, it is possible to provide a single electron level within the confining potential whereas at those same radii many hole levels would be crowded together within the confining potential created by a valence band offset. This result stems from the larger effective mass of the hole as compared with that of the electron.

QUANTUM DOT HETEROJUNCTIONS THAT FACILITATE STRAIN COMPENSATION

The formation of self-assembled quantum dots depends upon a strain induced two-dimensional to three-dimensional surface morphology [6]. The strain is produced by the lattice mismatch between the barrier material and the quantum dot material. In order to create a mini-band some measure of homogeneity must exist between the successive quantum dot layers. However, the strain may accumulate so that layers of coherent quantum dots may no longer be formed. In order for a high level of photon absorption to take place, the QD-IBSC must be formed with many quantum dot layers. In this paper quantum dot triads are presented that conform to the strain compensation technique of Akahane *et al.* [7]. The central point of this concept is that the lattice constant of the substrate must be in-between the lattice constants of the barrier and the quantum dot.

DESIGN RULES FOR A QUANTUM DOT INTERMEDIATE BAND SOLAR CELL

This section enumerates the design rules for selecting QD-IBSC materials triads (QD/barrier/substrate). The rules take into account electronic requirements, mechanical requirements and other practical considerations. The barrier material must have a bandgap, $E_{G,B}$, in the interval [1.43eV, 2.56eV], which approximately defines the > 60% efficiency regime as seen in Figure two found here [1]. In selecting the QD/barrier pair, there are three rules: the offset between the valence band edges, E_{CB}, must be negligible; the offset between the conduction band edges, E_{CB}, must be greater than $0.48 * E_{G,B} - 0.22$, which derives from a linear curve fit to the data within the > 60% regime of Figure 2 found here [1]; and the lattice mismatch between the two must be greater than 1%. The selection of a substrate is limited to those binary semiconductors that are commercially available. For the non-strain compensated triads the lattice constant of the barrier is fixed to that of a substrate. For the strain-compensated triads the lattice constant of the substrate is in-between the lattice constants of the barrier material and QD material.

The first and second group of results (see Tables 1 and 2) present triads whose barriers are lattice matched with their substrates. The third groups of results (see Table 3) present triads where for each triad the substrate's lattice constant is in-between the barrier material's lattice constants and the quantum dot material's lattice constants. Additionally, Tables 2 and 3 only include triads with barriers with direct bandgaps. This rule is inserted in order to improve the extent of light trapping. Materials with indirect bandgaps require phonon exchange to absorb photons. Further, the use of an indirect bandgap barrier material will require thicker devices to significantly trap light, which requires a longer duration of epitaxial growth.

The sole source of information used in selecting materials, based upon the above design rules, is a review paper authored by Vurgaftman *et al.* [8]. Their paper present bowing parameters to calculate the band edges as a function of lattice constants for the following III-V compound semiconductors: GaAs, GaSb, GaP, GaN, AlAs, AlSb, AlP, AlN, InAs, InSb, InP, and InN, as well as their ternary alloys.

RESULTS AND DISCUSSION

This section presents material triads that are found to meet the design requirements listed above. Table 1 lists non-strain compensated triads with thermodynamic efficiencies greater than 61.1% at maximum concentration. The barriers in Table 1 are indirect. Table 2 lists non-strain compensated triads with direct bandgap barriers. Table 3 lists strain-compensated triads with direct bandgap barriers. The latter portion of this section presents past research with the materials listed in Tables 1 through 3. Additional symbols that appear in these tables are as follows: ξ_{max} is the thermodynamic efficiency under maximum concentration, which is based upon the conditions that the value of E_{CV} is equal to the value of $E_{G,B}$ and that the value of E_{CI} is optimally placed; $E_{1,0}^{opt}$ is the location of the ground state energy that will set E_{CI} to its optimally position in a periodic lattice of quantum dots; and Δ a_{LC} is the lattice mismatch between the lattice constant of the barrier, $a_{LC,B}$ and the lattice constant of the quantum dot, $a_{LC,QD}$, which is defined as follows: Δ a_{LC} = $200*(a_{LC,QD} - a_{LC,B})/(a_{LC,QD} - a_{LC,B})$.

Table 1 lists two material triads that satisfy all the design rules for substrate/barrier lattice matched triads with efficiencies greater than 61.1%. The triads are {InAsSb, InPSb}/AlAsSb /InP. The lattice mismatches of 4.2% and 4.7% are sufficient to provide strain-induced self-organization of quantum dots in these materials.

	Promoted Triad One	Promoted Triad Two
Substrate	InP	InP
Barrier	$AlAs_{1-x}Sb_x$	$AlAs_{1-x}Sb_x$
Quantum dot	$InAs_{1-y}Sb_y$	$InP_{1-y}Sb_y$
X	0.44	0.44
Y	0.15	0.46
$E_{G,B}$ (eV)	1.93	1.93
E_{CB} (eV)	1.62	1.53
Δa_{LC} (%)	4.16	4.70
ξ_{max} (%)	61.8	61.1
$E_{1,0}^{opt}$ (eV)	0.56	0.53

Table 1. Information on two materials triads with which to implement a quantum dot intermediate band solar cell with negligible valence band offsets.

Table 2 lists material triads that satisfy all the design rules for substrate-barrier lattice matched triads and that have barrier materials with a direct conduction band. These triads may be written compactly as {InAsN, InAsP, InPSb}/AlInAs/InP. Within Table 2 there are triads with a wide range of lattice-mismatch and conduction band discontinuity with which to implement a QD-IBSC.

Dot Material	$E_{G,B}$ (eV)	E_{CB} (eV)	Δa_{LC} (%)	ξ_{max} (%)	$E_{1,0}^{opt}$ (eV)
$InAs_{0.9}N_{0.1}$	1.48	1.29	5.00	60.5	0.51
$InAs_{0.49}P_{0.51}$		0.57	5.19	60.5	0.51
$InP_{0.82}Sb_{0.18}$		0.56	5.50	60.5	0.51

Table 2. Information on QD-IBSC triads whose barriers are direct bandgap semiconductor compounds. For all the triads listed, the substrate is AlAs and the barrier is $GaAs_{0.98}Sb_{0.02}$.

Table 3 lists material triads that satisfy all the design rules for strain-compensated triads with a direct bandgap barrier. These triads may be written compactly as {InAsP, InPSb}/{AlInAs, GaAsSb, GaInAs}/InP. Not shown in Table 3 are three other triads that met the design rules, but were not included because they contain quantum dots composed of an alloy with a dilute nitride: InAsN/{GaAsSb, GaInAs}/InP and InPN/GaAsP/GaAs. Triads with dilute nitrides will not be considered because growth of these materials is still highly developmental. Most of the triads listed in Table 3 contain a range of molar concentrations that meet the design rules. These concentrations are given as well as the range of several important design parameters.

The remainder of this section discusses previous work with the material systems given in Tables 1 through 3. There are instances of $InAs_{1-y}Sb_y$ quantum dot growth with the following barrier materials: InAs (y~0.3) [9], GaAs (y~0.1) [10], InGaAs (y~0.1) [10], $InP_{0.24}As_{0.76}$ (y = [0.13, 0.2]) [11], $InP_{0.75}Sb_{0.25}$ (y=0.15) [12] and InP [13]. There are also instances of $InAs_{1-y}P_y$ quantum dot growth. Carlsson *et al.* produce samples (y~0.08) with dot heights centered around 5 nm [14]. Faradjev produced three QD samples with different pre-growth morphologies formed on InP [15]. One of these samples has QD with bimodal height distribution (~6 nm and ~30 nm). A second sample has QD with a unimodal height distribution (40 nm) with a sharp photoluminescence peak near 1200 nm. Rebeiro *et al.* present InAsP QD embedded in GaAs [16]. By controlling the phosphine flux, they present samples with different alloy compositions. They measure dot diameters/heights of 13/2.6 nm in one sample and 20/2.9 nm in another. In addition, there are instances of $InAs_{1-y}N_y$ quantum dot growth. Jang *et al.* produce five periods of InAsN QD on GaAs [17]. They record a peak in the photoluminescence spectrum at 1300 nm at room temperature. Daniltsev *et al.* produce InAsN QD on GaAs and measure a quantum dot density of $5x10^{-9}$ cm^{-2} and an average height of 2.2 nm [18]. Schumann *et al.* produce InAsN QD with nitrogen compositions between 0% and 4.3% [19]. They find that an increase in the amount of nitrogen corresponds to larger QD.

			Quantum Dot Materials	
			$InAs_yP_{1-y}$	$InP_{1-y}Sb_y$
Barrier Materials	$GaAs_{1-x}Sb_x$ $x = [0, 0.06]$	y	[0.40, 0.68]	[0.15, 0.25]
		$E_{G,B}$ (eV)	[1.52,1.41]	
		E_{CB} (eV)	[0.52, 0.69]	[0.51, 0.64]
	$Ga_{1-x}In_xAs$ $x = [0, 0.08]$	y	[0.40, 0.52]	[0.15, 0.19]
		$E_{G,B}$ (eV)	[1.52, 1.40]	
		E_{CB} (eV)	[0.52, 0.53]	~ 0.51
	$Al_{1-x}In_xAs$ $x \sim 0.50$	y	~ 0.40	~ 0.15
		$E_{G,B}$ (eV)	~ 1.58	
		E_{CB} (eV)	~ 0.59	~ 0.58

Table 3. Information on strain-compensated QD-IBSC triads whose barriers are direct bandgap semiconductor compounds. All triads are grown on InP.

CONCLUSIONS

Quantum dot intermediate band solar cell material triads (quantum-dot/barrier/substrate) have been uncovered that yield thermodynamic conversion efficiencies of over 60% at maximum concentration. These material triads are selected based upon several design rules. The valence band offsets between the quantum dot material and barrier material are negligible, thus mitigating efficiency loss due to minibands formed by hole states. The conduction band offsets between the quantum dot materials and barrier materials are at least as large as the energy gap (between the conduction band and intermediate band) required for high efficiency conversion. The barriers of triads listed herein are either direct or indirect bandgap semiconductors. Direct bandgap are preferential as they have larger absorption coefficients, with respect to indirect bandgaps, thus permitting the epitaxial growth of thinner solar cells. The lattice constants of the substrates are either lattice-matched with their barriers or are in-between the lattice constants of their quantum dot materials and their barriers. Both of these are presented so as to accommodate various growth recipes for self-assembling quantum dots.

ACKNOWLEDGEMENTS

M.L. and C.H. acknowledge the support of NREL through contract XAT4-44277-01. A.M and A.L acknowledge the support of the European Commission by funding FULL-SPECTRUM (Ref. N: SES6-CT-2003-502620).

REFERENCES

[1] A. Luque et al., “Increasing the Efficiency of Ideal Solar Cells by Photon Induced Transitions at Intermediate Levels”, *Phys. Rev. Let.* **78**, 1997, pp. 5014-5017.

[2] A. Martí et al., “Quantum Dot Intermediate Band Solar Cell”, *28th IEEE PVSC, 2000*, pp. 940-943.

[3] A. Martí et al., “Partial Filling of a Quantum Dot Intermediate Band for Solar Cells”, *IEEE Trans. on Elec. Dev.* **48**, 2001, pp. 2394-2399.

[4] M.Y. Levy et al., “Calculation of the Band Properties of a Quantum Dot Intermediate Band Solar Cell with Hydrogenic Impurities”, *19th Euro. Photo. Conf.*, 2004.

[5] M. Y. Levy, Georgia Institute of Technology M.S. Thesis, (2004).

[6] W. Seifert et al., “In Situ Growth of Nano-Structures by Metal-Organic Vapour Phase Epitaxy”, *J. of Crystal Growth* **170**, (1997), pp. 39-46.

[7] K. Akahane et al., “Fabrication of Ultra-High Density InAs-Stacked Quantum Dots by Strain-Controlled Growth on InP(311)B Substrate,” *J. of Crystal Growth* **245**, (2002), pp. 31-36.

[8] I. Vurgaftman et al., “Band Parameters for III–V Compound Semiconductors and their Alloys”, *J. of Appl. Phys.* **89**, 2001, pp. 5815-5875.

[9] A. Krier et al., “Midinfrared Photoluminescence of InAsSb Quantum Dots Grown by Liquid Phase Epitaxy”, *Appl. Phys. Lett.* **77**, 2000, pp. 3791-3793.

[10] K. Suzuki et al., “Near 1.3 μm Emission at Room Temperature from InAsSb/GaSb Self-Assembled Quantum Dots on GaAs Substrates”, *Phys. Stat. Sol.* **224**, 2001, pp. 139-142.

[11] R.M. Biefeld et al., “Recent Advances in Mid-Infrared (3-6 μm) Emitters”, *Mat. Sci. and Eng.* **B51**, 1998, pp. 1-8.

[12] R.M. Biefeld et al., “The Growth of Infrared Antimonide-Based Semiconductor Lasers by Metal-Organic chemical vapor deposition”, *J. of Mat. Sci.* **13**, 2002, pp. 649-657.

[13] Y. Qiu et al., “Self-assembled InAsSb Quantum Dots on (001) InP Substrates”, *Appl. Phys. Lett.* **84**, 2004, pp. 1510-1512.

[14] N. Carlson et al., “Growth of Self-Assembled InAs and $InAs_xP_{1-x}$ Dots on InP by Metalorganic Vapour Phase Epitaxy”, *J. Crystal Growth* **191**, 1998, pp. 347-356.

[15] F.E. Faradjev, “Extremely Narrow Photoluminescence from the Ensemble of InAsP/InP Quantum Dots”, *Mat. Sci. and Eng.* **B95**, 2002, pp. 279-282.

[16] E. Ribeiro et al., “Optical and Structural Properties of InAsP Ternary Self-Assembled Quantum Dots Embedded in GaAs”, *Appl. Phys. Lett.* **81**, 2002, pp. 2953-2955.

[17] Y.D. Jang et al., “InAsN/GaAs Quantum Dots with an Intense and Narrow Photoluminescence Peak at 1.3 μm”, *Physica E* **7**, 2003, pp. 347-356.

[18] V.M. Daniltsev et al., “InGaAsN/GaAs QD and QW Stuctures Grown by MOVPE”, *J. Crystal Growth* **248**, 2003 pp. 343-347.

[19] O. Schumann et al., “Morphology and Optical Propoerties of InAs(N) Quantum Dots”, *J. of Appl. Phys.* **96**, 2004, pp. 2832-2840.